

# New Estimates of the Sky Background for the HST Exposure Time Calculator

---

Mauro Giavalisco, Kailash Sahu and Ralph C. Bohlin  
October 9, 2002

---

## ABSTRACT

*We present new spectra of the optical and near-IR sky background radiation visible to Hubble Space Telescope (HST) instruments. This background includes contribution from both the zodiacal light and the Earthshine light, as well as geocoronal lines. The spectrum of the zodiacal light is obtained by reddening and normalizing that of the Sun so that it fits measures of background radiation taken in a region near the north ecliptic pole at 0.45, 0.5, 0.606, 0.814, 1.25 and 2.2  $\mu\text{m}$  with HST/WFPC2 and COBE/DIRBE. The Earthshine spectrum is derived from the solar spectrum at optical and near-IR wavelengths and is based on direct IUE measures in the UV. These spectra provide better agreement with available observations than previous versions, and are useful for calculating the background expected during observations with HST. They have been included in the data base of the Exposure Time Calculators (ETC) of HST instruments. Since the intensity of the background varies depending on the specific situations encountered during observations, such as the angle between the line of sight and the plane of the ecliptic or with the Earth's limb, we have implemented a suite of choices for the normalization of the spectra that should cover the range of conditions encountered in most observing programs.*

---

## Introduction

The Exposure Time Calculator (ETC) is the primary software tool for predicting the performances of HST instruments and for verifying the feasibility of proposed observations. Together with the sensitivity of the detectors, the transmittance and/or reflectivity of the

optics, and the passbands of the spectral elements (filters and dispersors), an accurate estimate of the spectral energy distribution of background light visible to the instruments is critical to the robustness of the simulations carried out by the ETC.

The three major contributors to the total HST sky background at UV through near-IR wavelengths are the zodiacal light, the Earthshine light and the geocoronal emission lines. Near-IR instruments, such as NICMOS and WFC3 are also sensitive to the thermal emission produced by the telescope and by the instrument's assembly, which become increasingly important components at the longer wavelengths and eventually dominate the background.

This Instrument Science Report presents improved estimates of the spectral energy distribution of the zodiacal light and Earthshine light at UV through near-IR wavelengths and discusses how to normalize their intensity to reproduce a number of observations made at different wavelengths with a number of telescopes and instruments. A separate ISR will deal with the thermal background for the upcoming WFC3. The new zodiacal and Earthshine spectra presented here have been incorporated in the ETC module of the recently released Astronomy Proposal Tool (APT), as well as in the previous CGI Web-based versions, which are still being used.

## **The Zodiacal Background**

The zodiacal background light is solar radiation reflected by dust in the inner solar system. Leinert et al. (1998) discuss the properties of the zodiacal background in great detail. By comparing available measurements of diffuse background at optical and infrared wavelengths to the spectrum of the solar radiation, they conclude that the spectrum of the zodiacal light is redder than the solar one and derive its shape by introducing a reddening correction to the solar spectrum of an amount appropriate to reproduce the observations. At the North Ecliptic Pole, the surface brightness of the zodiacal light is  $1.81 \times 10^{-18}$  erg  $\text{cm}^{-2} \text{s}^{-1} \text{\AA}^{-1} \text{arcsec}^{-2}$ , which corresponds to a V-band surface brightness (magnitudes are expressed in the HST  $f\text{-}\lambda$  system, see Koorneef et al. 1985) of  $23.3 \text{ mag/arcsec}^2$ , a value that Leinert et al. (1998) adopt to normalize their spectrum. Incidentally, this is also the normalization that has been traditionally used for the zodiacal spectrum used in previous versions of HST ETCs (e.g. see the STIS and WFPC2 Handbooks).

Aldering (2002) re-analyzed the Leinert et al. (1998) prescription for the zodiacal spectrum and compared it to recent observational data from HST and from COBE/DIRBE measures. The HST data are measures of background light at 0.450, 0.606 and 0.814  $\mu\text{m}$ , respectively, taken from the HDF-N survey (Williams et al. 1996; see also the HDF team's Web page, <http://www.stsci.edu/ftp/science/hdf/logs/MASTERLOG>), while the COBE/

DIRBE measures are at 1.25 and 2.2  $\mu\text{m}$  (Gorjian et al. 2000; Wright et al. 2001). In all cases the observed values have been rescaled to the North Ecliptic Pole (NEP) using the relationship provided by Leinert et al. (1998). Table 1 lists both the raw measures and the scaled NEP values. Aldering found an overall good agreement between the new (NEP-rescaled) data, Leinert's original V-band measure at the NEP, and Leinert's reddened solar spectrum. The agreement with the data could be further improved by adopting a slightly higher normalization (by 0.01 dex or 0.025 mag) of the spectrum and a slightly less overall reddening correction at  $\lambda > 0.5$  micron (by  $\sim 20\%$ ) than the Leinert et al. original prescription. These differences are well within the overall uncertainties of the measures and of the methodology adopted to model the spectrum and rescale the data at the NEP.

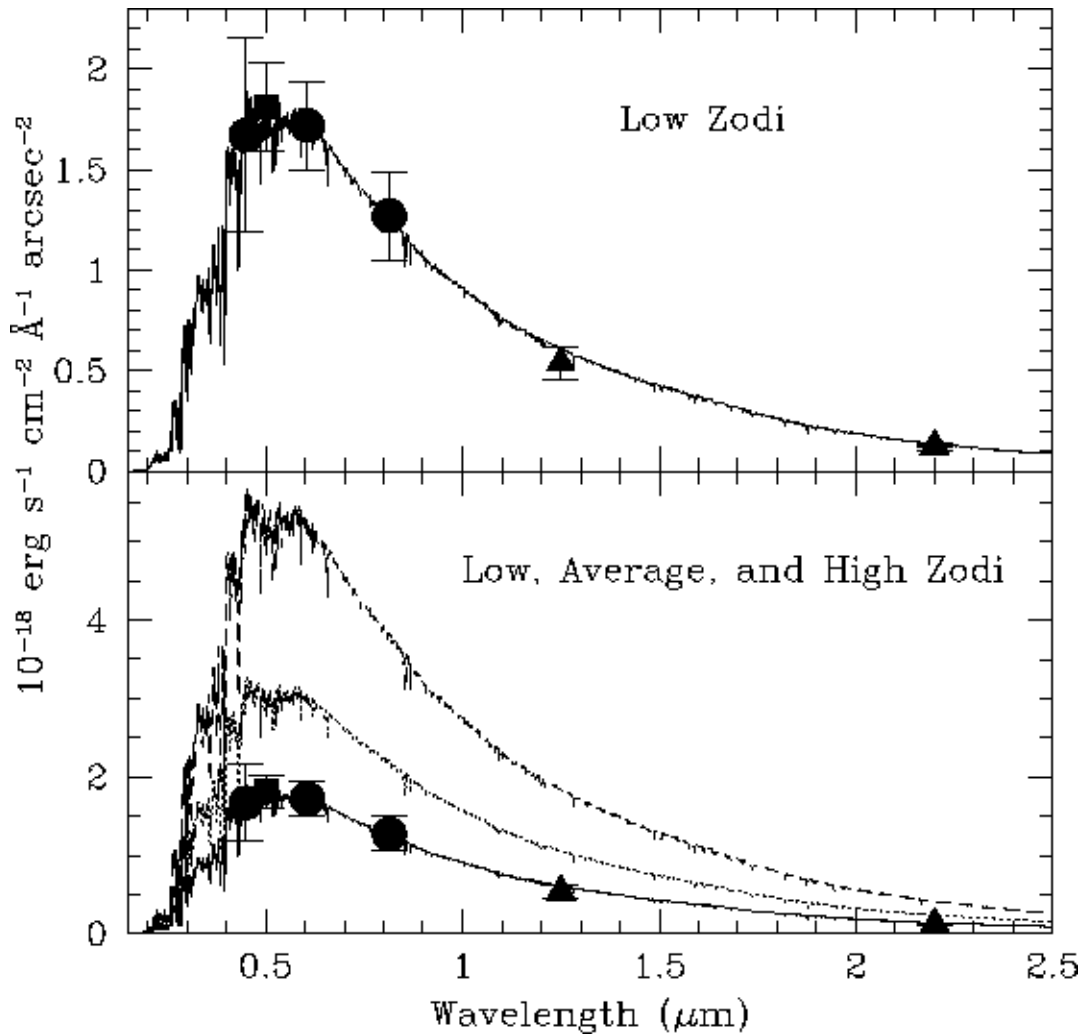


**Figure 1. Upper panel.** The spectrum of the zodiacal background light at the NEP compared to broad-band observations from the ground and HST observations. The circles are data at 0.450, 0.606 and 0.814  $\mu\text{m}$ , respectively from the HDF; the square is Leinert et al. (1998) measure at 0.5  $\mu\text{m}$ , and the triangles are measures from COBE/DIRBE at 1.25 and 2.2  $\mu\text{m}$ . **Lower panel.** The comparison between the intensity of the three adopted normalizations of the zodiacal background light. The lowest normalization is the one relative to the NEP, and it is shown together with the broad-band data points discussed above.

Aldering's description of the spectrum of the zodiacal background is adopted for use with the HST ETC because of the very good overall agreement with diverse data over the spectral range relevant to HST instruments. The model, normalized at  $0.50 \mu\text{m}$ , is analytical approximated as

$$\frac{f(\lambda)}{f(0.50\mu\text{m})} = 1.0 + 0.90 \ln\left(\frac{\lambda}{0.50\mu\text{m}}\right) \quad \text{for } \lambda < 0.5 \mu\text{m}$$

and

$$\frac{f(\lambda)}{f(0.50\mu\text{m})} = 1.0 + 0.48 \ln\left(\frac{\lambda}{0.50\mu\text{m}}\right) \quad \text{for } 0.5 < \lambda < 2.5 \mu\text{m}$$

Figure 1 shows the spectrum, which is obtained by reddening a solar spectrum from Colina, Bohlin & Castelli (1996) with the prescription by Leinert (1998) and with the revised normalization and reddening introduced by Aldering (2002). The figure also shows the HST (circles) and COBE/DIRBE background measures (triangle) together with Leinert et al. (1998)'s original point in the V band (square). The measures are also reported in Table 1, which lists both the observed surface brightness specific intensity as well as the value scaled to the NEP position. We note that this spectrum is in general good agreement with the model discussed by Stiavelli (2001), which is only marginally smaller at near-IR wavelengths.

Wavelength ( $\mu\text{m}$ )	Observed background ( $\text{erg sec}^{-1} \text{cm}^{-2} \text{\AA}^{-1}$ $\text{arcsec}^{-2}$ )	NEP flux density ( $\text{erg sec}^{-1} \text{cm}^{-2} \text{\AA}^{-1}$ $\text{arcsec}^{-2}$ )	$1-\sigma$ uncertainty ( $\text{erg sec}^{-1} \text{cm}^{-2} \text{\AA}^{-1}$ $\text{arcsec}^{-2}$ )	Source
0.500	$1.81 \times 10^{-18}$	$1.81 \times 10^{-18}$		Leinert et al. (1998)
0.450	$1.87 \times 10^{-18}$	$1.67 \times 10^{-18}$	$0.48 \times 10^{-18}$	HDF Team
0.606	$1.93 \times 10^{-18}$	$1.72 \times 10^{-18}$	$0.22 \times 10^{-18}$	HDF Team
0.814	$1.42 \times 10^{-18}$	$1.27 \times 10^{-18}$	$0.22 \times 10^{-18}$	HDF Team
1.25	$7.26 \times 10^{-19}$	$5.37 \times 10^{-19}$	$0.83 \times 10^{-19}$	Wright et al. 2001; Aldering 2002
2.2	$1.67 \times 10^{-19}$	$1.26 \times 10^{-19}$	$0.06 \times 10^{-18}$	Gorjian et al. 2000; Aldering 2002
2.2	$1.62 \times 10^{-19}$	$1.20 \times 10^{-19}$	$0.18 \times 10^{-19}$	Wright et al. 2001; Aldering 2002

**Table 1.** Measures of the zodiacal background. Except for Leinert's original one, all measures are scaled to their equivalent value at the NEP using the prescription of Leinert et al. (1998).

The spectrum shown in Figure 1 is the minimum zodiacal background observable by HST (the “low zodi light”). To simulate the effect of observing in regions other than the NEP, in the current version of the HST ETC we have elected to adopt two additional values of the overall normalization of the spectrum, namely  $V=22.7$  and  $V=21.1$ , to represent a “medium zodi” and a “high zodi” light, respectively. This approximation neglects the dependence of the zodi spectrum with the solar elongation, which is probably appropriate if the scattering function is a unique function of the scattering angle (Aldering 2002). Future releases of the HST ETC will include the possibility to calculate the background as a function of the celestial coordinates of the targets and the position of the Sun during the requested time for the observations.

### **The Earthshine Background**

At UV-optical wavelengths, e.g.  $\lambda < 4000 \text{ \AA}$ , the Earthshine radiation is due to residual air-glow and solar radiation reflected by the earth, which is independent on the underlying surface because the optical depth to the surface is large (Cox et al. 1987). The reflected radiation, therefore, is characterized by a solar spectrum modified by the albedo of the Earth. At longer wavelengths the reflected radiation depends on the underlying surface, and Cox et al. (1987) discussed the case of sunlit desert sand, water and clouds light, which provide a good description of the surface of the Earth as seen by HST. Because the light from sunlit cloud largely dominates the other two terms (that of the sand by a factor of  $\sim 2$ , and that of the sea water by a factor of  $\sim 100$ ; see Cox et al. 1987), particularly at redder wavelengths, and has a solar spectrum, we have approximated the spectrum of the total Earthshine as solar in shape, as well. This approximation conservatively over-estimates the spectrum (since the solar spectrum is redder than that of reflected light from sand and sea water) and because in most observing situations, the total background is dominated by the zodiacal light, and deviation from the solar spectral shape of sea water and sand reflected are smaller than the stochastic fluctuations of the intensity of the sunlit clouds’ reflected light due to randomly varying cloud coverage underlying the spacecraft. The Earthshine provides the dominant term to the total background only in observing conditions where the limb angle is small (e.g.  $\theta < 20$  degrees in presence of clouds), particularly during the day part of the orbit. In such a situation, fluctuations to the total intensity of Earthshine due to random cloud coverage dominate the deviations from the solar shape of the reflected light of sand and sea water.

Below  $4000 \text{ \AA}$ , however, the albedo of the Earth introduces significant deviations from the solar spectral shape; previous version of the Earthshine spectrum adopted in various HST ETCs used a spectrum derived from IUE observations. We composed a new Earthshine spectrum by matching IUE spectral observations of the Earth at  $\lambda < 4000 \text{ \AA}$  (Cox et al. 1987) and an appropriately rescaled solar spectrum at  $\lambda > 4000 \text{ \AA}$ . This synthetic spectrum is shown in Figure 2.

The intensity of the Earthshine cannot be precisely predicted because of the randomly varying cloud coverage. Therefore, in analogy with the zodiacal light case, four different values of the overall normalization are chosen to represent corresponding “typical” observational situations of low, average, high and very high Earthshine background. Our assumptions might not represent a realistic situation in some actual observations, however. Observers who simulate observations whose outcome critically depends on the intensity of the Earthshine must request the “LOW SKY” option during the scheduling of their program, or choose a conservative value for the Earthshine intensity. It is useful to remind, at this purpose, that an important case where the Earthshine may dominate the sky background is when observing in the Continuous Viewing Zone (CVZ) near the orbital pole. Future releases of the ETC will offer users the opportunity to specify their own value of the normalization of the spectrum of both the zodiacal and Earthshine light.

The spectrum shown in Figure 2 has the “High Earth” value of the normalization, which corresponds to a limb angle of 38 degree. The HST ETC will also include an “Extremely High Earth”, corresponding to a limb angle of 24 degrees, which has twice the intensity as the “High Earth” case. In turn, the “Average Earth” normalization is 50% of the value of the “High” one and corresponds to a limb angle of ~50 degree. Higher limb angles result in a negligible intensity of the Earthshine; the HST ETCs use zero Earthshine for the “Low Earth” case.

The Earthshine spectrum of Figure 2 does not include the geocoronal emission lines. However, these lines provide the major component of the flux of the Earthshine radiation that is observed at UV wavelengths, even in a broad bandpass, and must, therefore, be included in a realistic calculation of the background. The geocoronal emission is confined to a very few lines in the UV wavelengths. The brightest geocoronal line is Ly $\alpha$  at 1216 Å and other, weaker lines are O I 1302 Å, O I 1356 Å and O II 2470 Å. The strength of the O I 1302 Å line rarely exceeds 10% of the Lyman alpha one, while the other lines are much weaker. Observations with IUE found that the strength of the geocoronal Ly $\alpha$  varies between about ~2 and ~30 kiloRayleighs (between  $6 \times 10^{-14}$  and  $9.2 \times 10^{-13}$  erg cm<sup>-2</sup> sec<sup>-1</sup> arcsec<sup>-2</sup>), depending on the time of observations and the position of the target relative to the Sun. The contribution of this emission line to the Earthshine can be minimized by the special requirement "SHADOW". The ETC incorporates a value of 20 kiloRayleighs ( $6.1 \times 10^{-13}$  erg cm<sup>-2</sup> sec<sup>-1</sup> arcsec<sup>-2</sup>) for the geo-coronal Lyman emission when the background is specified as "High" or "Extremely High". The geocoronal emission lines have thermal Doppler widths, which can be calculated from in-situ measures of the temperature of the Earth's upper atmosphere (e.g. Finlayson-Pitts & Pitts 1999). The strength and the width of the various geocoronal emission lines used in the HST ETC are listed in Table 2.

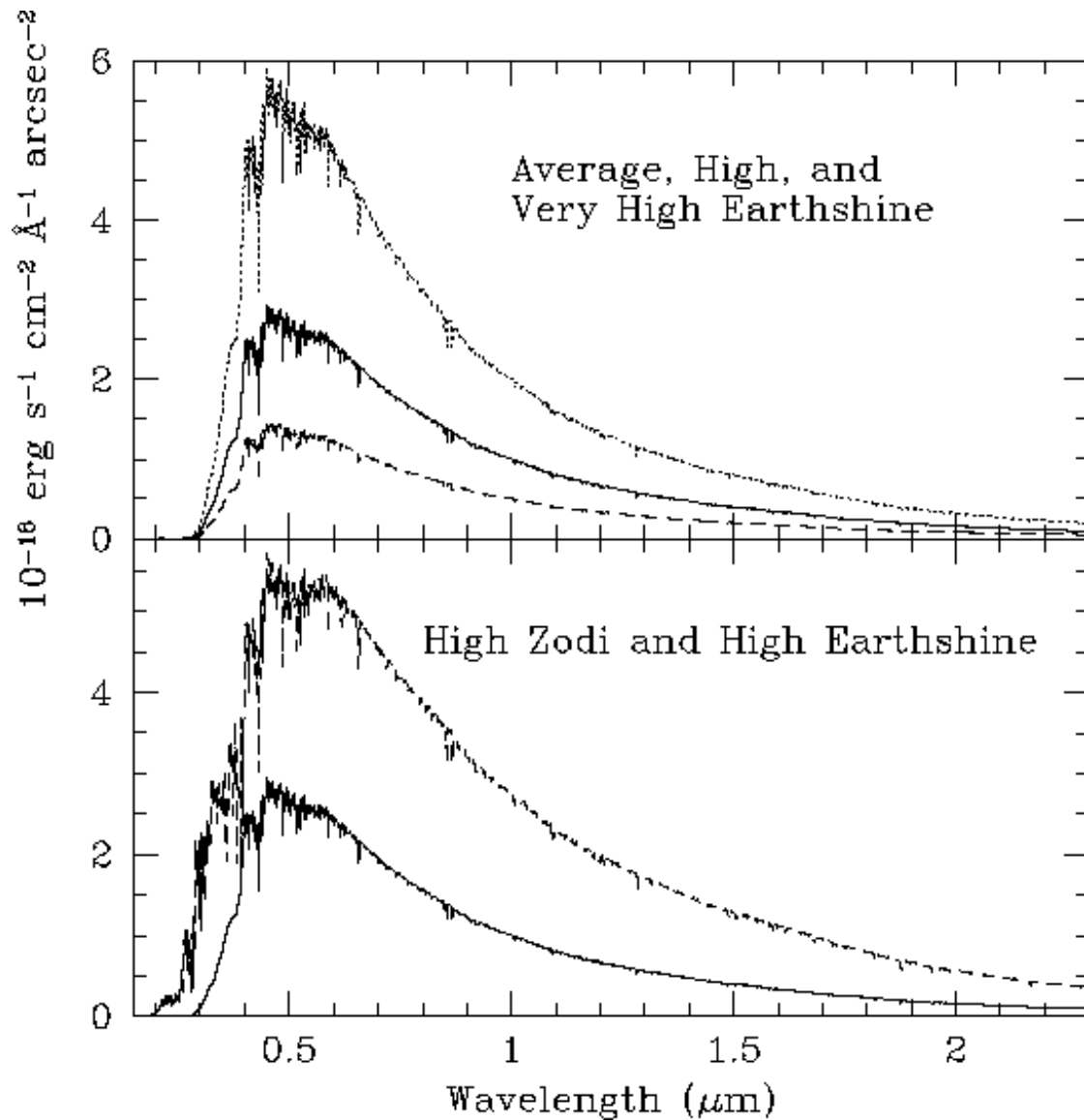


**Figure 2. Upper Panel:** the comparison between the Average, High and Very High spectra of the Earthshine. The normalization of the Average and Very High spectra differ by a factor 1/2 and 2, respectively, from that of the High one. The intensity of the Low Earthshine background is assumed zero. **Lower Panel:** the comparison between the High Zodi and High Earthshine spectra, where the Zodi light dominates.

Wavelength (Å)	Line Width (Å)	High value (erg sec <sup>-1</sup> cm <sup>-2</sup> arcsec <sup>-2</sup> )	Average value (erg sec <sup>-1</sup> cm <sup>-2</sup> arcsec <sup>-2</sup> )	Low value (erg sec <sup>-1</sup> cm <sup>-2</sup> arcsec <sup>-2</sup> )
1216	0.04	6.1x10 <sup>-13</sup>	3.05x10 <sup>-13</sup>	6.1x10 <sup>-14</sup>
1304	0.013	5.7x10 <sup>-14</sup>	2.85x10 <sup>-14</sup>	3.8x10 <sup>-16</sup>
1356	0.013	5.0x10 <sup>-15</sup>	2.50x10 <sup>-15</sup>	3.0x10 <sup>-17</sup>
2471	0.023	3.0x10 <sup>-15</sup>	1.50x10 <sup>-15</sup>	1.5x10 <sup>-17</sup>

**Table 2.** Wavelength, line width and intensity of the geocoronal emission lines

## Conclusion

We discussed revised models of the spectral energy distribution of background radiation that affects HST observations. The dominant contributor to the background in most observations is the zodiacal light; and the revised model of its spectrum is in excellent agreement with ground-based, HST and COBE direct observations of the background. The Earthshine light become the dominant source of background whenever the telescope limb angle is very small (e.g. less than ~25 degree). For example, an important case where the Earthshine may dominate the sky background is when observing in the Continuous Viewing Zone (CVZ) near the orbital pole. The revised Earthshine spectrum discussed here provides an adequate representation of this background, since the driving factor in the uncertainty on the intensity of the background is the total amount of light reflected by the Earth more than its spectral shape, which varies randomly. The contribution of geocoronal emission lines is a major fraction of the UV radiation coming from the Earth. Our background intensities are now used in the HST ETCs, including both the current CGI, Web based versions, as well as the module of the Astronomer Planning Tool (APT) that is about to be released.

## References

- Aldering, G. 2002, "SNAP Sky Background at the North Ecliptic Pole," LBNL Report 51157
- Finlayson-Pitts, B.J., & Pitts, J.N. Pitts, 1999, "Chemistry of the Upper and Lower Atmosphere: Theory, Experiments, and Applications", Academic Press
- Colina, L., Bohlin, R.C., & Castelli, F. 1996, AJ, 112, 307

Coorneef, J., Bohlin, R., Buser, R., Horne, K., Turnshek, D., 1986 “Synthetic Photometry and the Calibration of the Hubble Space Telescope”, Highlights of astronomy, Proceedings of the Nineteenth IAU General Assembly, Delhi, India (Dordrecht, D. Reidel Publishing Co.), Vol. 7, p. 833

Proceedings of the XIX I.A.U. General Assembly  
Cox, C.R., Bohlin, R.C., Griffith, R.E., & Kelsall, K. 1987, STScI

Gorjian, V., Wright, E.L., & CHary, R.R. 2000, ApJ, 536, 550

Leinert, C., et al. 1998, A&AS, 127, 1

Stiavelli, M. 2001, STScI Instrument Science Report, WFC3-ISR 2002 - 02

Williams, R.E. 1996, AJ, 112, 1335

Wright, E.L. 2001, ApJ, 496, 1